Deep 10 Micron Imaging of M87

Eric S. Perlman[1,2], William B. Sparks[3], James Radomski[4], Chris Packham[4],
R. Scott Fisher[5], Robert Piña[4], & John A. Biretta[3]

Gemini Preprint #80

1. Department of Physics, Joint Center for Astrophysics, University of Maryland-Baltimore County, 1000 Hilltop Circle, Baltimore, MD 21250, USA
2. Department of Physics and Astronomy, Johns Hopkins University, 3400 North Charles Street, Baltimore, MD 21218, USA
3. Space Telescope Science Institute, 3700 San Martin Drive, Baltimore, MD 21218, USA
4. Department of Astronomy, University of Florida, 211 SSRB, Gainesville, FL 32611, USA
5. Gemini Observatory, 670 N. A'Ohoku Place, Hilo, HI 96720, USA

Deep 10 Micron Imaging of M87[1]

Eric S. Perlman [2,3], William B. Sparks [4], James Radomski [5], Chris Packham [5], R. Scott Fisher [6], Robert Piña [5], & John A. Biretta [4]

perlman@jca.umbc.edu

ABSTRACT

We analyze a 10.8 μm image of M87, obtained with the Gemini 8m telescope + OSCIR. The image has $< 0.5''$ resolution and represents 7 hours of observing time, making it the deepest high-resolution mid-IR image ever. The nucleus is resolved, and we also detect five optically bright knots in the jet. The spectral energy distributions of these features are entirely consistent with synchrotron radiation; we find little evidence of thermal emission from a dusty torus. Four faint jet regions are below the noise level of these observations. We also find evidence for diffuse galactic emission.

1. Introduction

Besides being the nearest giant elliptical galaxy ($d = 16$ Mpc, Tonry 1991, corresponding to 78 pc/arcsec), M87 has several features which make it a critical object for understanding galaxies' life cycles. These include: (1) energetic nuclear emissions from an accretion disk (Ford et al. 1994, Harms et al. 1994); (2) dusty, filamentary Hα lanes, extending over 1

[2]Department of Physics, Joint Center for Astrophysics, University of Maryland-Baltimore County, 1000 Hilltop Circle, Baltimore, MD 21250, USA

[3]Department of Physics and Astronomy, Johns Hopkins University, 3400 North Charles Street, Baltimore, MD 21218, USA

[4]Space Telescope Science Institute, 3700 San Martin Drive, Baltimore,MD 21218, USA

[5]Department of Astronomy, University of Florida, 211 SSRB, Gainesville, FL 32611, USA

[6]Gemini Observatory, 670 N. A'Ohoku Place, Hilo, HI 96720, USA

[1]Based on observations obtained at the Gemini Observatory, which is operated by Association of Universities for Research in Astronomy, Inc., under a cooperative agreement with the NSF on behalf of the Gemini partnership: the National Science Foundation (United States), the Particle Physics and Astronomy Research Council (United Kingdom), the National Research Council (Canada), CONICYT (Chile), the Australian Research Council (Australia), CNPq(Brazil) and CONICET(Argentina).

kpc (Jarvis 1990, Sparks, Ford & Kinney 1993, Sparks et al. 2000); and (3) a 25″ (2 kpc) long relativistic jet which feeds lobes many times larger than the galaxy (Sparks, Biretta & Macchetto 1996; Biretta et al. 1999; Perlman et al. 1999, 2001; Marshall et al. 2001).

Several components can contribute to mid-IR emission from an active galaxy: (1) galactic dust; (2) photospheric emission from the stellar population; (3) thermal dust emission from the nuclear torus; and (4) synchrotron radiation from jets or lobes. Because of M87's large black hole mass ($\approx 3 \times 10^9 M_\odot$; Marconi et al. 1997), its torus might be resolvable in ground based observations, as unified schemes (Urry & Padovani 1995) predict a size scale of 10^{5-6} Schwarzschild radii (20-200 pc or $0.3'' - 3''$ for M87's black hole mass and distance).

2. Observations and Data Reduction

We observed M87 with Gemini-North, using OSCIR[7], the University of Florida's mid-IR imager/spectrometer. OSCIR uses a Boeing 128×128 Si:As blocked-impurity-band detector (0.089″/pixel), sensitive between 8-25 μm. We used the broad N-band filter, centered at 10.8 μm ($\nu = 2.78 \times 10^{13}$ Hz) with a 5.3 μm bandpass (50% cut on/off).

Because of the $11'' \times 11''$ field of view, we rotated the instrument support structure so that the jet fell along a chip diagonal, and used two pointing centers, 4″ and 14″ from the nucleus. Observations were done in a "chop-and-nod" sequence to subtract time-variable sky background, using a 30″ north-south chop to minimize galaxy contributions. On 3 May 2001, we observed M87 for 5 hours (1.25 hours on-source), in good conditions (no cirrus and low precipitable water content): 3 at the nuclear position (45 minutes on-source) and 2 at the jet position (30 minutes on-source). Four more hours (1 hour on-source) were obtained at the nuclear position on 10 May 2001. Of those, two had good sky conditions, but the last two suffered from cirrus giving rise to a much higher, variable background.

Hourly images of a nearby star were obtained for PSF comparison. Flux calibration was obtained using α Lyr ($N = 0.00$), β Leo ($N = 1.84$) and α Boo ($N = -3.14$) as standards (Cohen et al. 1992, 1999; Tokunaga 1984). Absolute errors in flux calibration were obtained by measuring the fluxes of the core in individual hours' data; this leads to an estimate of 4% if only the 3 May data are included, but 10% if the 10 May data are also included.

The data were reduced with IDL routines written for the OSCIR observation structure and data format. Chopped pairs that were obviously compromised by high electronic noise, cirrus or other problems were discarded. Electronic noise was removed from one jet

[7]For information on OSCIR, see http://www.gemini.edu/sciops/instruments/oscir/oscirContents.html.

image via Fourier filtering, which transformed the data into a frequency space map where high freuqency noise was easily identified and removed. Images from 10 May suffered from variable sky conditions which could not be fully removed by chopping and nodding. The residual sky was modeled with a third order polynomial constructed from the images. This model was then subtracted from the 10 May images to account for the variable background. We combined the nuclear images in 10-nod-set groups, to better track pointing drift and account for differential atmospheric refraction. The nuclear and jet images were registered by assuming that the positions of the nucleus and knot C were identical at H and N bands.

All data from 3 May and the two cirrus-free hours on 10 May were used for the final image, shown in Figure 1 along with the core's radial profile. The PSF is $0.46''$ FWHM. Figure 2 compares the 10.8 μm image with HST 1.6 μm and VLA 2 cm images (Perlman et al. 2001). Fluxes for the core and jet components labelled in Figure 2 are given in Table 1.

3. What is the Nature of the Nuclear Mid-IR Emission?

The nature of M87's nuclear emission has been a continuing controversy. Figure 3 shows the from core flux Table 1, an 11.7 μm Keck/LWS point (Whysong & Antonucci 2001), earlier mid-IR photometry (§5), the optical power-law from Sparks et al. (1996) and a 230 K blackbody. Also shown on Figure 3 is a continuous injection (Heavens & Meisenheimer 1987) synchrotron emission model, fitted to earlier radio,optical and X-ray data (Sparks et al. 1996, Marshall et al. 2001). As shown, the Gemini and Keck points agree with the synchrotron model, indicating that the nuclear N-band emission is consistent with emission from the innermost regions of the jet. The derived break frequency is $\nu_b = 2.8 \times 10^{12}$ Hz.

Figure 1b compares the radial profile of M87, to the PSF star. As can be seen, the nucleus of M87 is slightly resolved, with a significant excess above the PSF at radii $> 0.6''$. This emission could possibly be associated with the torus, but with the current image we cannot make this statement with any confidence. This component constitutes $7.3 \pm 1.2\%$ of the nuclear flux, corresponding to an upper limit of 1.2 mJy on the 10.8μm torus emission.

4. What is the Nature of the Mid-IR Emission from the Knots?

As seen in Figure 2, we detect five of the nine optically bright knots in the jet. In the radio, optical and X-ray, these emit synchrotron radiation (Perlman et al. 2001, Marshall et al. 2001). If indeed their mid-IR emissions are synchrotron in nature, one would expect: (1) similar morphology in near-IR, mid-IR and radio; and (2) fluxes which agree with synchrotron

models. With these data, we can verify prediction (1) for knots A, B and C.

Figure 4 shows the knot fluxes (Table 1), compared to synchrotron models fit to radio, optical and X-ray data (Marshall et al. 2001), using the spectral aging formalism of Kardashev (1962) and Pacholczyk (1970). Since the 10.8 μm fluxes for all knots agree fairly well with the models, we interpret the mid-IR emission from the knots as synchrotron radiation.

5. Extended Galactic Emission?

We have added to the core fluxes in Figure 3, points from IRAS observations (Moshir et al. 1990) and previous ground-based photometry (Rieke & Low 1972, Rieke & Lebofsky 1978, Puschell 1981). All were made with large apertures: $> 1'$ for the IRAS points, $6''$ for the Rieke & Low (1972) and Rieke & Lebofsky (1978) points and $35''$ for the Puschell (1981) point. Importantly, extrapolated (using the models in §4) fluxes for jet regions were subtracted from these points as appropriate. The large-aperture points all lie well above the Gemini and Keck fluxes for the nuclear source. This might seem obvious confirmation of the presence of galactic mid-IR emission from M87. However, the nucleus of M87 is variable by up to a factor 2 in the optical (Tsvetanov et al. 1998), so we must be more careful.

To further examine this issue, we extracted radial profiles from archival ISOCAM images at 6.7, 12 and 14.3 μm, masking the jet in the process. As shown in Figure 5, M87's mid-IR emission extends to at least $40''$. Unfortunately it is impossible to extract fluxes from the ISO data because the core and jet are not resolved. This emission is probably stellar in origin given the lack of a PAH feature (Rigopoulou et al. 1999) in the ISOPHOT-S spectrum.

6. Discussion

As the product of 7 hours of 8m telescope time, the Gemini image is the deepest ground-based mid-IR image ever. The 5σ point-source detection limit is 0.36 mJy. By comparison, the Keck/LWS image (Whysong & Antonucci 2001; §3) represents 15 minutes of telescope time (96 s on-source), and was taken with a narrower filter (1 μm).

Recent observations (Moorwood 1999, Laurent et al. 2000, Alonso-Herrero et al. 2001, Whysong & Antonucci 2001, Radomski et al. 2001, Meisenheimer et al. 2001), indicate significant torus emission in many but not all active galaxies. Whysong & Antonucci (2001) make an apt comparison to Cyg A and Cen A, which show bright tori (Cen A: Rydbeck et al. 1993, Mirabel et al. 1999; Cyg A: Conway 1999, Whysong & Antonucci 2001, Radomski et al. 2001). M87 is intermediate in jet power between Cyg A and Cen A (Owen et al. 2000,

Chiaberge et al. 2001, Wan et al. 2000; although Reynolds et al. 1996a estimate the jet power of M87 nearly 2 orders of magnitude lower than do Owen et al.). Moreover, its black hole ($M = 3 \times 10^9 M_\odot$, Marconi et al. 1997), is $\sim 10\times$ more massive than Cen A's (Marconi et al. 2001), so that its ratio of jet power to black hole mass is *higher* by over an order of magnitude (no good estimate for Cyg A's black hole mass exists in the literature). Yet our results correspond to an upper limit on the ratio of torus to radio luminosity for M87, which is three orders of magnitude lower than either Cen A or Cyg A. Thus with current data it is not possible to draw broad generalizations regarding the contribution of obscuring matter to the AGN's energy budget, or its connection to either accretion rate or jet luminosity.

Reynolds et al. (1996b) modeled M87's nuclear regions in terms of an advection-dominated accretion flow (ADAF; Narayan & Yi 1995; Narayan, Yi & Mahadevan 1996). Their model requires an accretion rate about 3 orders of magnitude lower than the Eddington rate. However, it is not consistent with M87's observed properties, in particular: (1) a much lower ν_b than observed, and (2) nuclear X-ray emission dominated by thermal bremsstrahlung, which is contrary to the nuclear X-ray spectrum (Marshall et al. 2001), and variability (Harris et al. 1997). The observation that the nuclear emission in all wavebands is jet-dominated, probably lowers the estimate of disk power and hence accretion rate for M87 by at least an order of magnitude, although an exact assessment requires detailed analysis.

It is extremely interesting that the nuclear ν_b value is 3-5 orders of magnitude lower than those seen in the knots 80-1000 pc from the nucleus ($10^{15.5} - 10^{17.5}$ Hz, Perlman et al. 2001, Marshall et al. 2001). Moreover, X-ray synchrotron emitting electrons have lifetimes ~ 10 yrs (Biretta et al. 1991), so *in situ* particle acceleration in the knots is required. Further evidence for this likely shock related process, is found in optical and radio polarimetry (Perlman et al. 1999) as well as sharp spectral changes in knots (Perlman et al. 2001).

Importantly, each of the issues explored in this paper requires a much deeper image not only at 10.8 μm but also 20 μm to fully elucidate. This would allow us to fit mid-IR spectral indices and/or dust temperatures to each component. Such observations, both of M87 and also of other nearby AGN, are of crucial importance for 10m-class telescopes.

We thank the Gemini-North Observatory staff, particularly J.-R. Roy, C. Aspin and W. Shook. We thank C. Telesco for help with data acquisition and interesting discussions. E. S. P. acknowledges discussions with M. Begelman, J. Krolik, C. Reynolds, H. Netzer and S. Malhotra for help with the ISO data. E. S. P. acknowledges support from NASA LTSA grant NAG 5-9997 and HST grant GO-7866. W. B. S. and J. A. B. acknowledge HST grants GO-5941, GO-7274, GO-8048 and GO-8140. C. P., R. S. F. and J. R. acknowledge support from NSF, the Gemini Observatory and the Florida Space Grant Consortium.

REFERENCES

Alonso-Herrero, A., Quillen, A. C., Simpson, C., Efstathiou, A., & Ward, M., 2001, AJ, 121, 1369

Biretta, J. A., Sparks, W. B., & Macchetto, F., 1999, ApJ, 520, 621

Biretta, J. A., Stern, C. P., & Harris, D. E., 1991, AJ, 101, 1632

Chiaberge, M., Capetti, A., & Celotti, A., 2001, MNRAS, in press, astro-ph/0105159

Cohen, M., Walker, R. G., Barlow, M. J., & Deacon, J. R., 1992, AJ, 104, 1650

Cohen, M., Walker, R. G., Carter, B., Hammersley, P., Kidger, M., & Noguchi, K., 1999, AJ, 117, 1864

Conway, J. E., 1999, in "Highly Redshifted Radio Lines", ed. C. L. Carilli, S. J. E. Radford, K. M. Menten, & G. I. Langston (Provo: PASP), p. 259

Ford, H. C., et al., 1994, ApJ, 435, L27

Harms, R. J., et al., 1994, ApJ, 435, L35

Harris, D. E., Biretta, J. A., & Junor, W., 1997, MNRAS, 284, L21

Heavens, A., & Meisenheimer, K., 1987, MNRAS, 225, 335

Jarvis, B. J., 1990, A & A 240, L8

Kardashev, N. S., 1962, Soviet Astronomy – AJ 6, 317.

Laurent, O., et al., 2000, A & A 359, 887

Marconi, A., Axon, D. J., Macchetto, F. D., Cappetti, A., Sparks, W. B., Crane, P., 1997, MNRAS, 289, L21

Marconi, A., Capetti, A., Axon, D., Koekemoer, A., Macchetto, D., & Schreier, E., 2001, ApJ, 549, 915

Marshall, H. L., Miller, B. P., Davis, D. S., Perlman, E. S., Canizares, C. R., Harris, D. E., & Biretta, J. A., 2001, ApJ, in press

Meisenheimer, K., Haas, M., Müller, S. A. H., Chini, R., Klaas, U., & Lemke, D., 2001, A& A, 372, 319

Mirabel, I. F., et al., 1999, A & A, 341, 667

Moorwood, A. F. M., 1999, in The Universe As Seen by ISO, eds. P. Cox & M. F. Kessler, ESA-SP 427, p. 825

Moshir, M., et al., 1990, The IRAS Faint Source Catalogue, Version 2.0

Narayan, R., Yi, I., 1995, ApJ, 452, 710

Narayan, R., Yi, I., Mahadevan, R., 1996, A & A S, 120, 287

Owen, F., Eilek, J. A., & Kassim, N. E., 2000, ApJ, 543, 611

Pacholczyk, A. G., 1970, Radio Astrophysics (San Fransisco: Freeman).

Perlman, E. S., Biretta, J. A., Sparks, W. B., Macchetto, F. D., & Leahy, J. P., 2001, ApJ, 551, 206

Perlman, E. S., Biretta, J. A., Zhou, F., Sparks, W. B., & Macchetto, F. D., 1999, AJ 117, 2185

Puschell, J. J. 1981, ApJ, 247, 48

Radomski, J. T., Pina, R. K., Packham, C., Telesco, C. M., Tadhunter, C. N., 2001, ApJ, submitted,

Reynolds, C. S., Fabian, A. C., Celotti, A., & Rees, M. J., 1996a, MNRAS, 283, 873

Reynolds, C. S., di Matteo, T., Fabian, A. C., Hwang, U., & Canizares, C. R., 1996b, MNRAS, 283, L111

Rieke, G. H., & Lebofsky, M. J., 1978, ApJ, 220, L37

Rieke, G. H., & Low, F. J., 1972, ApJ, 176, L95

Rigopoulou, D., Spoon, H. W. W., Genzel, R., Lutz, D., Moorwood, A. F. M., & Tran, Q. D., 1999, AJ, 118, 2625

Rydbeck, G., Wiklind, T., Cameron, M., Wild, W., Eckart, A., Genzel, R., & Rothermel, H., 1993, A& A 270, L13

Sparks, W. B., Baum, S. A., Biretta, J., Macchetto, F. D., Martel, A. R., 2000, ApJ, 542, 667

Sparks, W. B., Biretta, J. A., & Macchetto, F., 1996, ApJ, 473, 254

Sparks, W. B., Ford, H. C., & Kinney, A. L., 1993, ApJ, 413, 531

Tokunaga, A. T., 1984, AJ, 89, 172

Tonry, J. L., 1991, ApJ, 373, L1

Tsvetanov, Z. I., et al., 1998, ApJ, 493, L83

Urry, C. M., & Padovani, P., 1995, PASP, 107, 803

Wan, L., Daly, R. A., & Guerra, E. J., 2000, ApJ, 544, 671

Whysong, D., & Antonucci, R., 2001, ApJL, submitted, astro-ph/0106381

10 Arcsec

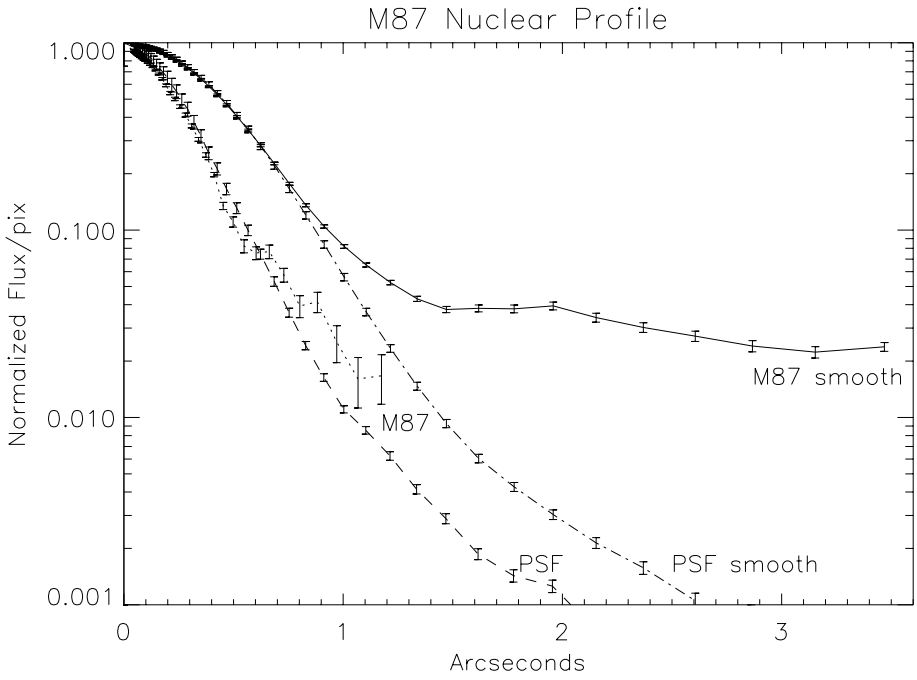

Fig. 1.— At top (Figure 1a), we show the final, mosaiced Gemini image. The image has been adaptively smoothed and rotated so that the jet is along the x axis. The core and several jet regions can clearly be seen. At bottom (Figure 1b), we show the radial profile of the core, compared to the PSF star, both unsmoothed and smoothed with a 3 pixel Gaussian. As can be seen, we do detect a faint extended component of the nuclear emission from M87.

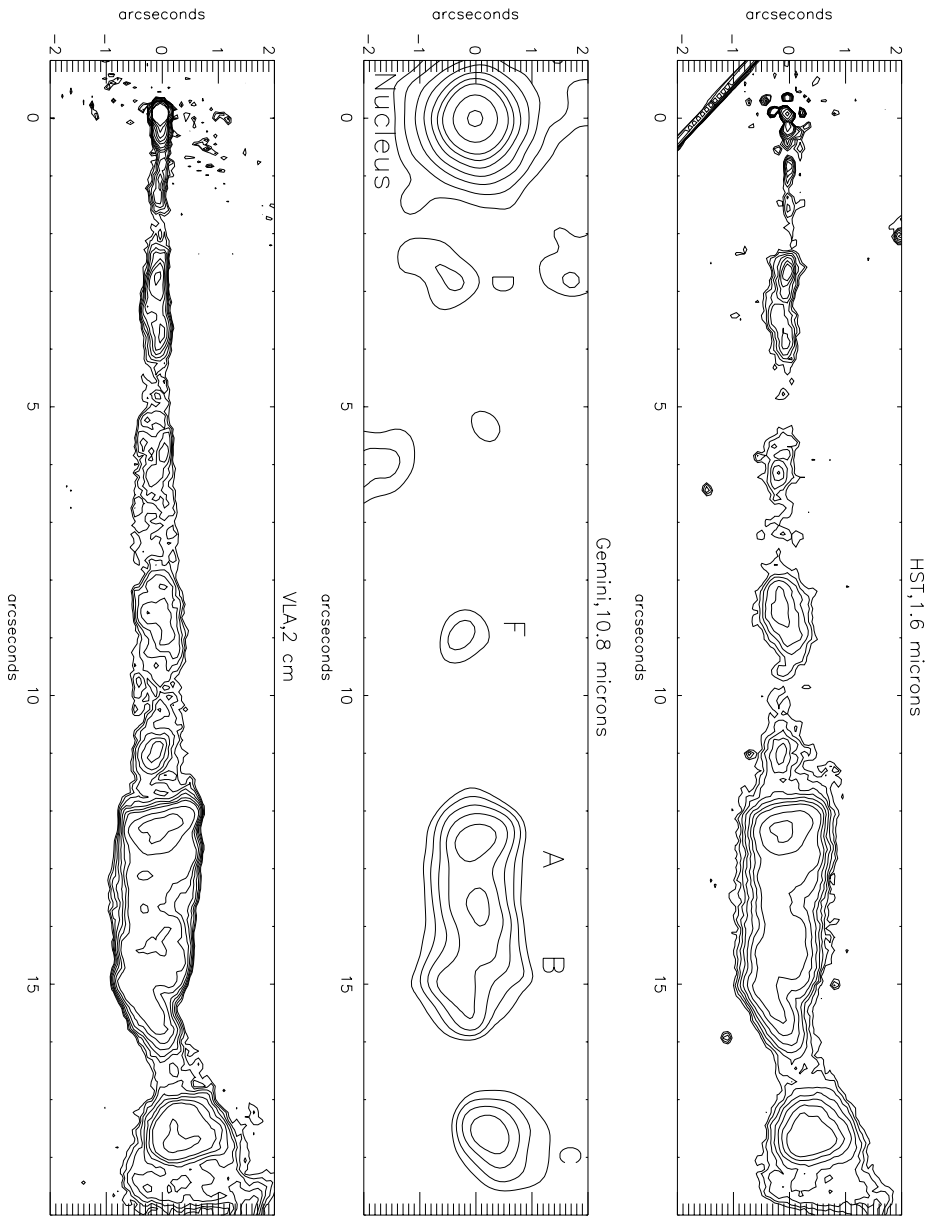

Fig. 2.— Here we show the Gemini 10.8 μm image (middle) of the M87 jet, compared with images taken with the HST at 1.6 μm (top) and with the VLA at 2 cm (bottom). Bright knot regions detected in the Gemini image are marked with the usual designations. The contours shown represent (1,1.4,2,2.8,4,5.7,8,16,32,64,128,256) times the 5σ rms noise level of each image. The diagonal noise in the HST image is an edge-of-field artifact. For comparison, the resolutions (FWHM) are $0.15''$ (HST and VLA) and $0.46''$ (Gemini).

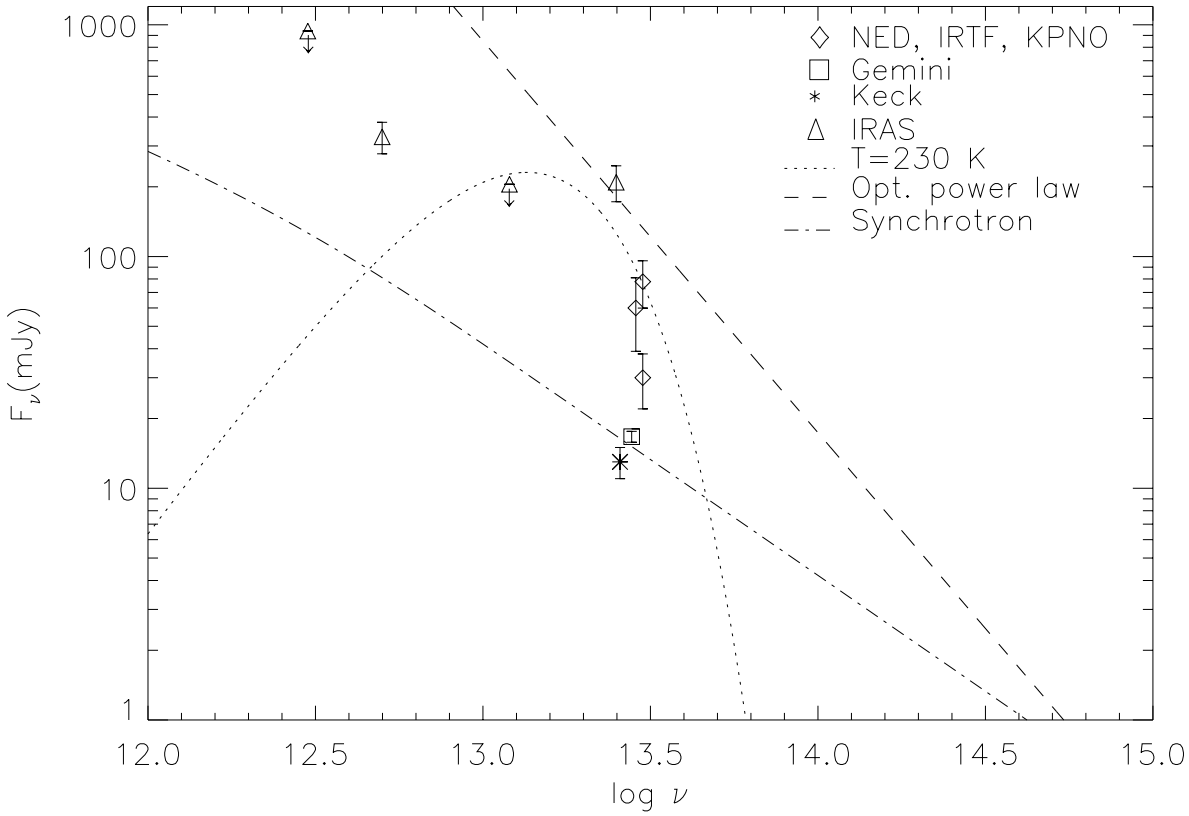

Fig. 3.— Recent mid-infrared photometry of the M87 nucleus, plotted along with large-aperture points from previous ground based and IRAS measurements. Also shown for comparison are the optical power law from Sparks et al. (1996), a 230K blackbody, and a synchrotron emission model. The nuclear emission is entirely consistent with synchrotron emission and there is no evidence for thermal emission from a dusty torus. However, significant additional flux is seen in larger aperture measurements. See §§3,5 for details.

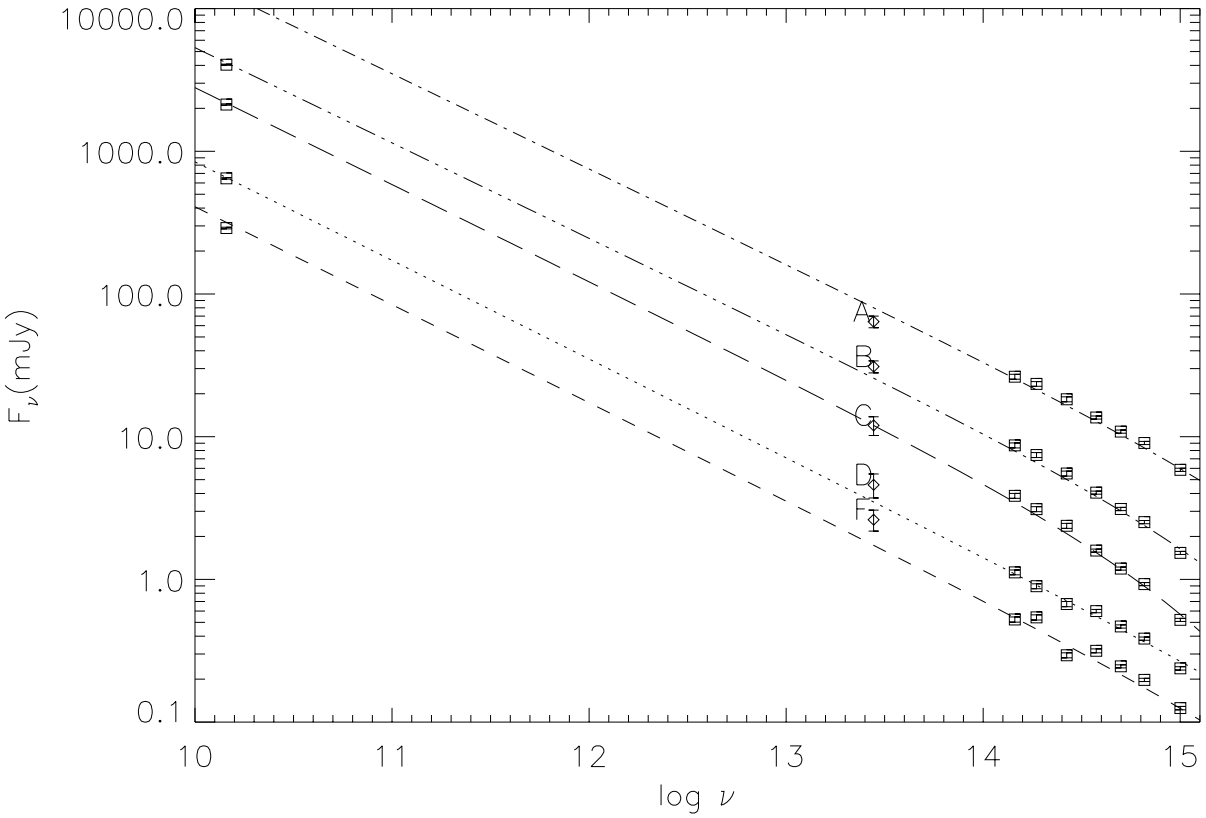

Fig. 4.— Radio-optical Spectral Energy Distributions for each of the knots we detect in the M87 jet. The knots have each been multiplied by an arbitrary factor for display purposes. The curves represent synchrotron models fit to radio-optical-X-ray data by Marshall et al. (2001). As can be seen, the mid-IR emission from the knots is consistent with synchrotron emission. See §4 for details.

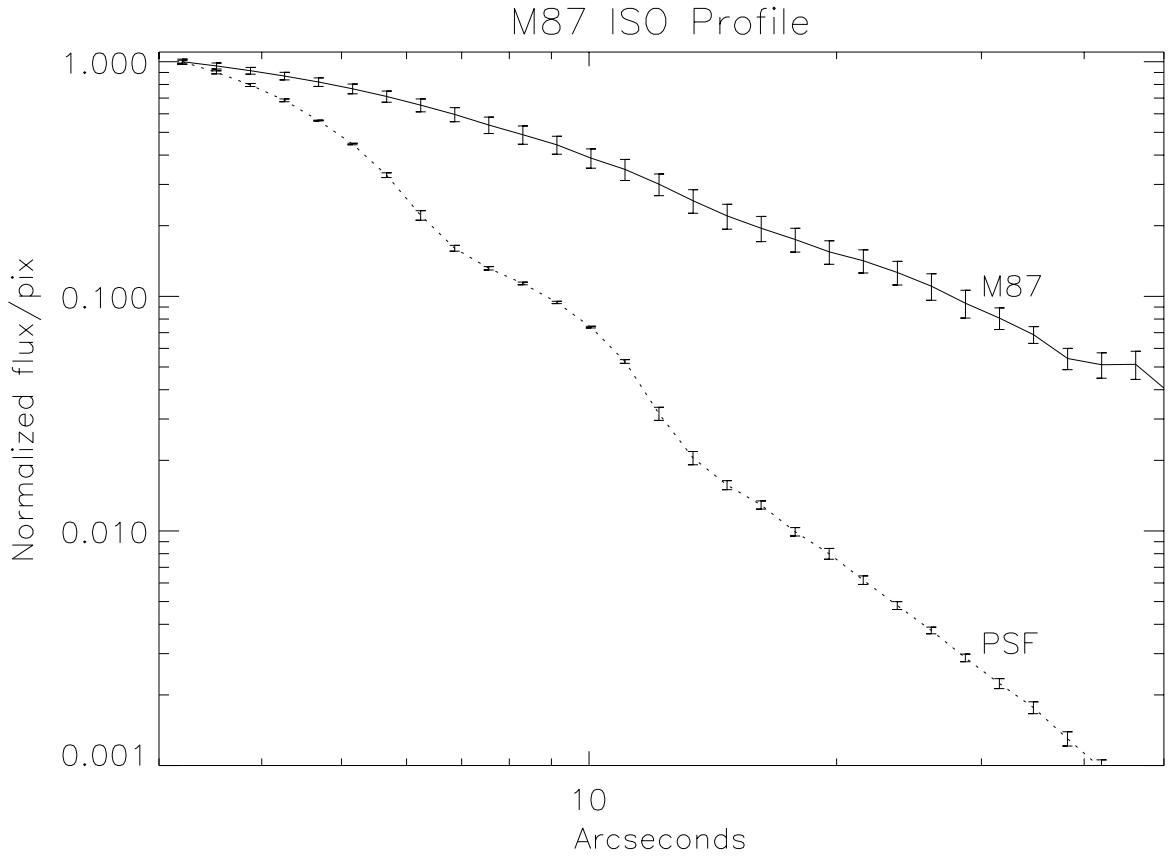

Fig. 5.— The radial profile of M87 at 14.3 μm from ISO data, compared with a theoretical PSF. As can be seen, the mid-IR extent of M87's galactic emission is $\gtrsim 40''$. See §5 for details.

Table 1. Fluxes of Jet Components

Component	Flux (mJy)
Nucleus	16.7 ± 0.9
Knot D	1.15 ± 0.22
Knot F	1.31 ± 0.22
Knot A	6.4 ± 0.6
Knot B	6.3 ± 0.6
Knot C	4.0 ± 0.6